

Surface Properties and Antibacterial Activity of Quaternized Polysulfones

Anca Filimon,¹ Ecaterina Avram,¹ Simona Dunca,² Iuliana Stoica,¹ Silvia Ioan¹

¹Petru Poni Institute of Macromolecular Chemistry, Iasi 700487, Romania

²Alexandru Ioan Cuza University, Faculty of Biology, Iasi 700506, Romania

Received 11 June 2008; accepted 2 November 2008

DOI 10.1002/app.29591

Published online 11 February 2009 in Wiley InterScience (www.interscience.wiley.com).

ABSTRACT: Novel quaternized polysulfones (PSFs) with two ionic chlorine contents were investigated, namely, their morphology and antimicrobial activity. Atomic force microscopy (AFM) studies on their membranes showed ordered domains, in which pores and nodules of different sizes and intensities were distributed. The charge density of the quaternized PSFs and the history of the membranes formed from solutions in solvent/nonsolvent mixtures influenced the different aspects of the surface images. The adhesion of *Esche-*

richia coli ATCC 10536 and *Staphylococcus aureus* ATCC 6538 microorganisms to solutions of the modified PSFs is discussed in correlation with the hydrophobic/hydrophilic properties of the studied polymers and microorganisms. © 2009 Wiley Periodicals, Inc. *J Appl Polym Sci* 112: 1808–1816, 2009

Key words: association; atomic force microscopy (AFM); biological applications of polymers; membranes; poly-electrolytes

INTRODUCTION

In recent decades, considerable attention has been devoted to the investigation of new applications of polysulfones (PSFs), mainly because of their specific properties. The literature shows that PSFs and their derivatives have been widely used as new functional materials in biochemical, industrial, and medical fields because of their structure and physical properties, such as their good optical properties, high thermal and chemical stabilities, mechanical strength, resistance to extreme pH values, and low creep.^{1–3} Their chain rigidity is derived from the relatively inflexible and immobile phenyl and SO₂ groups, whereas their toughness is derived from the connecting ether oxygen.⁴ Although these materials have excellent overall properties, their intrinsic hydrophobic nature precludes their use in membrane applications, which require a hydrophilic character. Therefore, such polymers should be modified to improve their performance for specific applications.^{5,6} The chemical modification of PSFs, especially the chloromethylation reaction, is a subject of considerable interest from both theoretical and practical points of view; there is interest in obtaining the

precursors for functional membranes, coatings, ion-exchange resins, ion-exchange fibers, and selectively permeable membranes.^{2,7,8} Functionalized polymers and chloromethylated and quaternized polysulfones (PSFQs) have evidenced several interesting properties that recommend them for a wide range of industrial and environmental applications.^{9–11} Quaternization with ammonium groups is an efficient method for increasing their hydrophilicity. Accordingly, these polymers can be used for multiple applications, for example, as biomaterials and semi-permeable membranes. Also, the different components of a block or graft copolymer may segregate in bulk to yield nanometer-sized patterns or mesophasic structures. Numerous applications involve nanodomain solids.¹² By matching the periodicity of the patterns with the wavelength of visible light, literature studies have demonstrated that block copolymers, including PSFs, act as photonic crystals. Segregated block copolymers, PSFs included, have been also used as precursors for the preparation of various nanostructures, including nanospheres, nanofibers, nanotubes, and thin membrane-containing nanochannels. Thin membranes containing nanochannels have been used as membranes, pH sensors, and templates for the preparation of metallic nanorods. Furthermore, in recent decades, blends of PSF or modified PSFs and other synthetic polymers have continued to be a subject of intense academic and industrial investigation because of their simplicity and effectiveness in the mixture of two different polymers for producing new materials.^{13,14}

Correspondence to: S. Ioan (ioan_silvia@yahoo.com).

Contract grant sponsor: Romanian National Council for Scientific Research in Higher Education; contract grant numbers: TD-548/2008, A-104GR/2008.

TABLE I
Ionic Chlorine Content (Cl_i), Structural Unit Molecular Weight (*m*₀), and Number-Average Molecular Weight (*M*_n) Values of the PSFQs

Sample	Cl _i (%)	<i>m</i> ₀	<i>M</i> _n
PSFQ1	2.15	479.47	42,000
PSFQ2	5.71	647.31	57,000

In such applications, the addition of functional groups to the PSF can enhance some properties of the material. For example, these groups can modify the hydrophilicity (which is of special interest for biomedical applications),¹⁵ antimicrobial action,¹⁶ and solubility characteristics^{17,18} to allow higher water permeability and better separation.^{19,20} In addition, functional groups are an intrinsic requirement for affinity, ion-exchange, and other specialty membranes.²¹

In previous publications, the synthesis^{22–24} and some solution properties^{17,18,25–28} of new PSFs have been presented. Studies have been carried out on the quaternization reaction of chloromethylated polysulfones (CMPSFs) for obtaining water-soluble polymers with various amounts of ionic chlorine. The conformational behavior in solution and the experimental and theoretical results of the preferential adsorption coefficients versus solvent composition have been discussed in correlation with the interaction parameters of PSFQs/mixed solvents.^{18,26} Surface wettability and hydrophilicity trends were also analyzed for biomaterials and semipermeable membrane applications.²⁸ In this study, atomic force microscopy (AFM) was used to investigate the morphological characteristics of PSFQ membranes obtained from solutions in different solvent/nonsolvent mixtures, and the results were correlated with the solution and hydrophilic/hydrophobic properties of the polymers. At the same time, the analysis of antibacterial activity, with *Escherichia coli* ATCC 10536 and *Staphylococcus aureus* ATCC 6538 microorganisms, may contribute to extending the possible applications of PSFQs membranes in biomedical domains.

EXPERIMENTAL

Materials

UDEL-1700 PSF (Union Carbide, Texas City, TX; number-average molecular weight = 39,000; weight-average molecular weight/number-average molecular weight = 1.625), a commercial product, was purified by repeated reprecipitation from chloroform and dried for 24 h *in vacuo* at 40°C before it was used in the synthesis of CMPSF. A mixture of commercial paraformaldehyde with an equimolar amount of chlorotrimethylsilane (Me₃SiCl) as a chloromethylation agent and stannic tet-

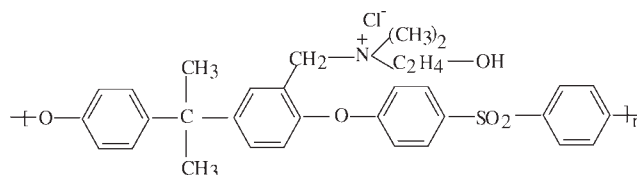
rachloride (SnCl₄) as a catalyst was used for the chloromethylation reaction of PSF at 50°C. The reaction time was varied from 24 to 140 h to obtain different substitution degrees of the CMPSFs.²² Finally, the samples were dried *in vacuo* at 40°C. CMPSF was dissolved in *N,N*-dimethylformamide (DMF) vacuum-distilled over P₂O₅, after which the *N,N*-dimethylethanolamine (DMEA) quaternized derivative was poured into the reactor. The reaction time was 48 h at 60°C.²⁴ The characteristics of the studied PSFQs are presented in Table I. The ionic chlorine and total chlorine contents were determined by potentiometric titration (Titrator TTT1C Copenhagen, Denmark) with 0.02N AgNO₃ aqueous solutions. The ratios between the ionic chlorine and the total chlorine contents showed that the quaternization reaction of the CMPSFs occurred with a transformation degree close to 96–98%. Thus, one may consider that almost all of the chloromethylene groups were quaternized.

The general chemical structure of PSFQ is presented in Scheme 1.

Antimicrobial activity tests

The *in vitro* antimicrobial activity of PSFQ1 and PSFQ2, assessed on two strains of bacteria, namely, *E. coli* (ATCC 10536) and *S. aureus* (ATCC 6538), by the disk-diffusion method (Kirby–Bauer) certificated by the National Committee on Clinical Laboratory Standards, was evidenced by the occurrence of an inhibition zone. The bacteria were preincubated for 18 h at 37°C.

An agar plate with pH 7.2–7.4 at room temperature was uniformly inoculated with the test microorganism with a sterile cotton swab, and disinfected steel discs were placed on the agar surface. Three milliliters from each PSFQ solution and also from the control sample, dimethyl sulfoxide (DMSO), were introduced into the discs. The plates were incubated at 37°C for 24 h. The growth of the microorganism and diffusion of the PSFQ solution occurred simultaneously, a circular zone of inhibition, in which the amount of polymer solution exceeded inhibitory concentrations, thus resulted. The diameter of the inhibition zone was a function of the amount of polymer present in the disk and of the microorganism susceptibility. Finally, the diameter of the inhibition clear zone was measured with a ruler.



Scheme 1 General structure of PSFQ.

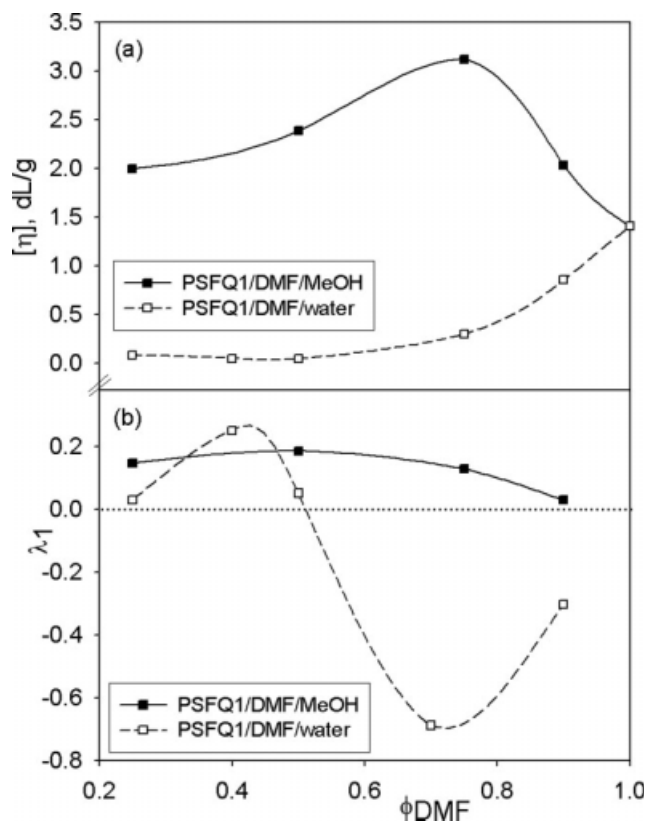


Figure 1 Influence of the DMF volume fraction (ϕ) on the (a) intrinsic viscosity ($[\eta]$) and (b) preferential adsorption (λ_1) for PSFQ1 in DMF/MeOH and DMF/water mixtures at 25°C.

AFM

AFM images were obtained on a SPM SOLVER Pro-M instrument (Zelenograd, Russia). A NSG10/Au Silicon tip with a 35-nm curvature radius and a 255-kHz oscillation mean frequency was used to investigate the membrane surface morphology. The apparatus was operated in semicontact mode over scan areas of $500 \times 500 \text{ nm}^2$, $3 \times 3 \mu\text{m}^2$, $5 \times 5 \mu\text{m}^2$, and $60 \times 60 \mu\text{m}^2$; 512×512 scan point size images were thus obtained. The used membranes were prepared from solutions of 20 g/dL concentration in DMF/methanol (MeOH) and DMF/water for PSFQ1 and in MeOH/DMF and MeOH/water for PSFQ2 at different composition ranges of these solvent mixtures. The polymer solutions were cast on flat glass and gradually oven-dried at different temperatures to control the solvent evaporation rate. Finally, the membrane was placed in a vacuum oven for 2 days at 50°C.

RESULTS AND DISCUSSION

Surface morphology

Some studies have reported that the chain shape of a polymer in solution could affect the morphology of the polymer in bulk.^{29–31} The PSFQs membranes

used in AFM were prepared with different solvent mixtures, including DMF/MeOH, DMF/water, MeOH/DMF, and MeOH/water. The solvent systems were selected as a function of the ionic chlorine content of PSFQ. Thus, DMF solvated PSFQ1 with an ionic chlorine content of 2.15% more intensely than the mixed DMF/MeOH and DMF/water solvents with high contents of MeOH and water, respectively. On the other hand, MeOH solvated PSFQ2 with an ionic chlorine content of 5.71% more strongly than the mixed MeOH/DMF and MeOH/water solvents with high contents of DMF and water, respectively.^{18,26} Figures 1 and 2 plot the modification of chain conformation from the variation of intrinsic viscosity with the composition of DMF for PSFQ1 and of MeOH for PSFQ2, respectively.

AFM was used to examine the film surfaces and to measure their surface topography. All of the images presented in Figures 3–5 were recorded under ambient conditions at different size scales to provide morphological details. Each micrograph shows that the membrane surface was not smooth, existing in ordered domains, in which there were distributed pores and nodules of different sizes and intensities.

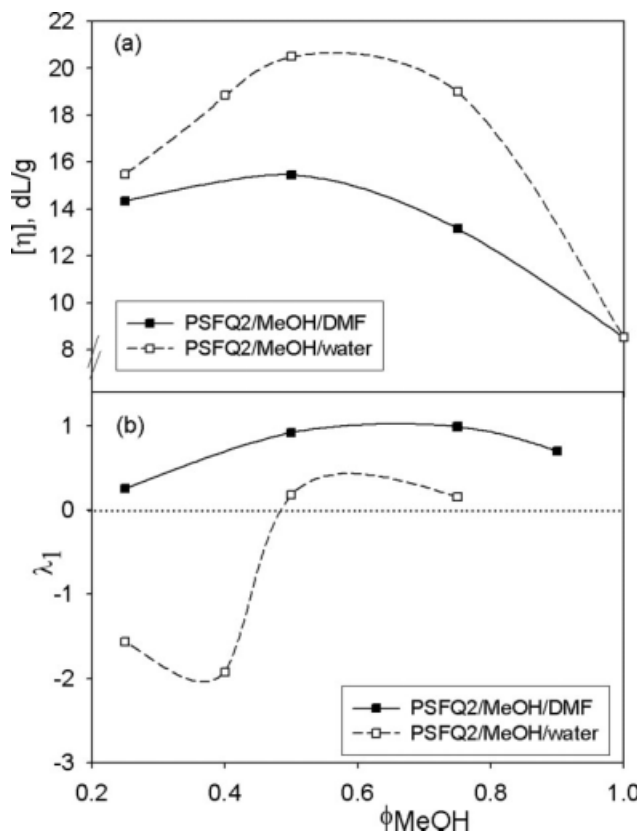


Figure 2 Influence of the MeOH volume fraction (ϕ) on the (a) intrinsic viscosity ($[\eta]$) and (b) preferential adsorption (λ_1) for PSFQ2 in MeOH/DMF and MeOH/water mixtures at 25°C.

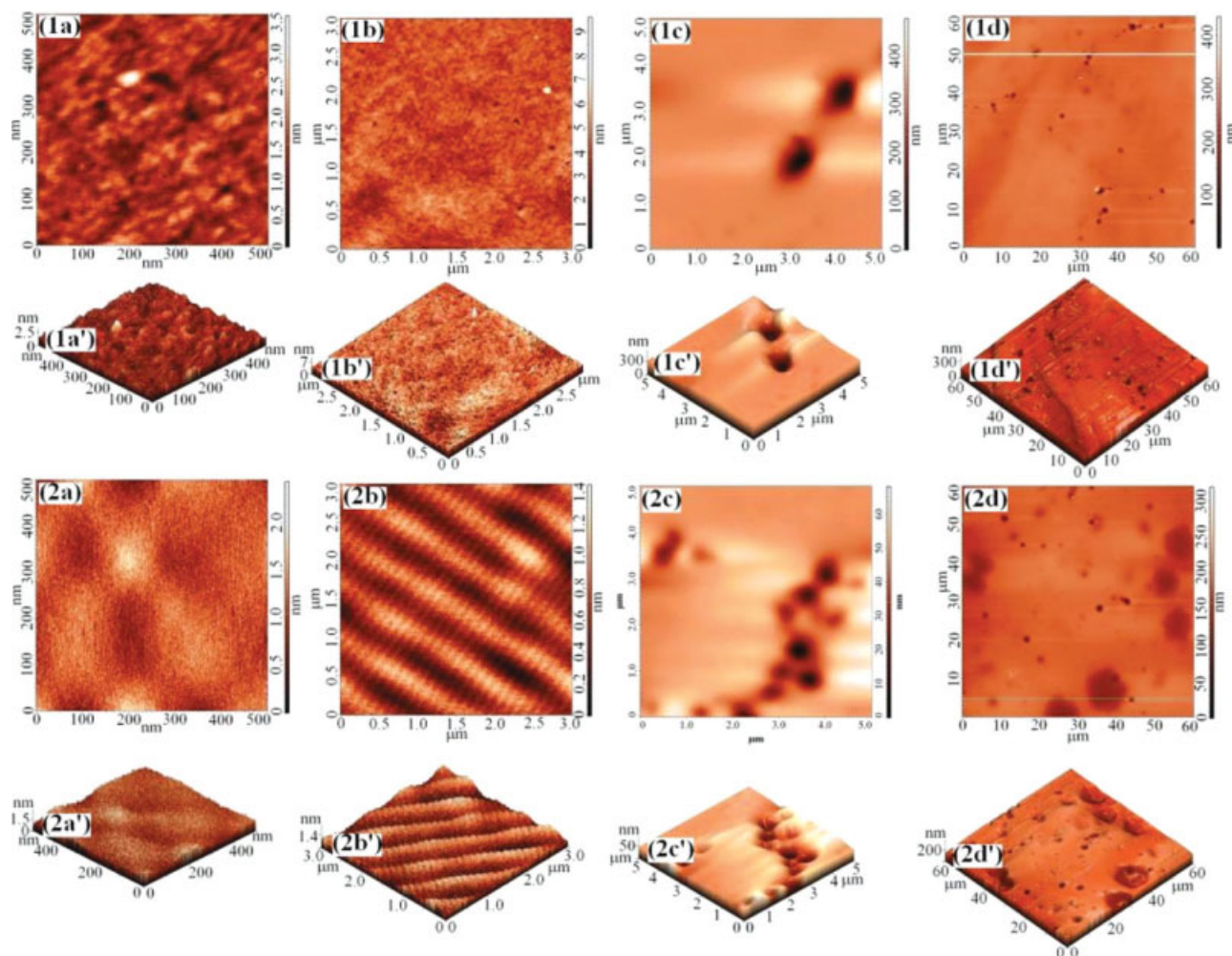


Figure 3 AFM images of the PSFQ1 membranes obtained from different DMF/MeOH solvent mixtures: (1) 60/40 DMF/MeOH: (a) 2D scanned area = $500 \times 500 \text{ nm}^2$, (b) 2D scanned area = $3 \times 3 \mu\text{m}^2$, (c) 2D scanned area = $5 \times 5 \mu\text{m}^2$, (d) 2D scanned area = $60 \times 60 \mu\text{m}^2$, (a') 3D image of (a), (b') 3D image of (b), (c') 3D image of (c), and (d') 3D image of (d) and (2) 20/80 DMF/MeOH: (a) 2D scanned area = $500 \times 500 \text{ nm}^2$, (b) 2D scanned area = $3 \times 3 \mu\text{m}^2$, (c) 2D scanned area = $5 \times 5 \mu\text{m}^2$, (d) 2D scanned area = $60 \times 60 \mu\text{m}^2$, (a') 3D image of (a), (b') 3D image of (b), (c') 3D image of (c), and (d') 3D image of (d). [Color figure can be viewed in the online issue, which is available at www.interscience.wiley.com.]

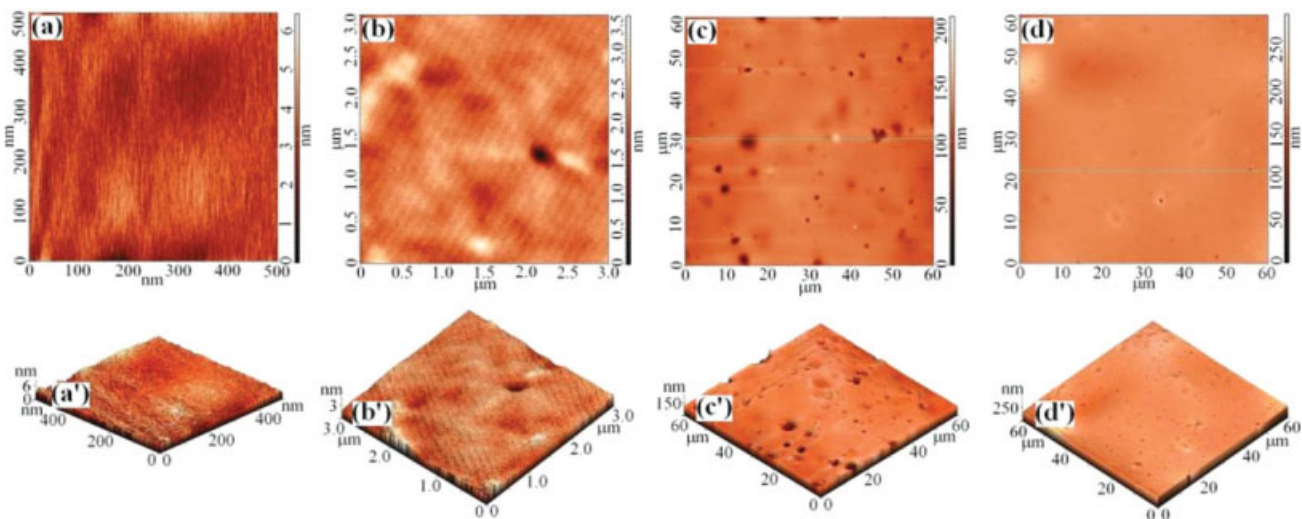


Figure 4 AFM images of the PSFQ1 membranes obtained from the (a) 60/40 DMF/water solvent mixture, 2D scanned area = $500 \times 500 \text{ nm}^2$; (b) 60/40 DMF/water solvent mixture, 2D scanned area = $3 \times 3 \mu\text{m}^2$; (c) 60/40 DMF/water solvent mixture, 2D scanned area = $60 \times 60 \mu\text{m}^2$; (d) 40/60 DMF/water solvent mixture, 2D scanned area = $60 \times 60 \mu\text{m}^2$; (a') 3D image of (a); (b') 3D image of (b); (c') 3D image of (c), and (d') 3D image of (d). [Color figure can be viewed in the online issue, which is available at www.interscience.wiley.com.]

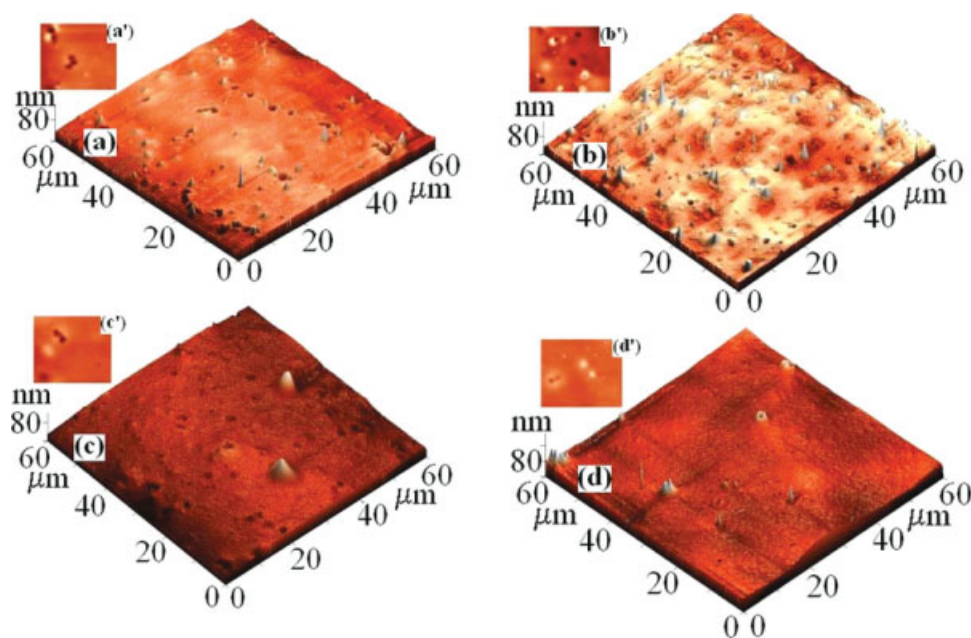


Figure 5 3D AFM images of the PSFQ2 membranes obtained from the (a) 60/40 MeOH/DMF, (b) 20/80 MeOH/DMF, (c) 60/40 MeOH/water, and (d) 20/80 MeOH/water solvent mixtures. (a'), (b'), (c'), and (d') represent the domains of the 2D AFM images with scanned areas of $60 \times 60 \mu\text{m}^2$, corresponding to the 3D images of (a), (b), (c), and (d). [Color figure can be viewed in the online issue, which is available at www.interscience.wiley.com.]

According to our data, increasing the nonsolvent content in the casting solutions favored modification of the ordered domains, more visibly in images with a $500 \times 500 \text{ nm}^2$ or $3 \times 3 \mu\text{m}^2$ scanning area. Thus, the average surface roughness in the $3 \times 3 \mu\text{m}^2$ scanning area decreased from 0.354 nm for the PSFQ1 membranes obtained in 60 DMF/40 MeOH [Figs. 3(1b,1b')] in two-dimensional (2D) and three-dimensional (3D) AFM images, respectively] to 0.193 nm for the PSFQ1 membranes realized in 20 DMF/80 MeOH [Fig. 3(2b,2b'), in 2D and 3D AFM images, respectively].

Also, the AFM images from Figure 3, for a more extended scanning area, showed that increasing the nonsolvent content favored the increase of the pore number and of their characteristics, such as area,

volume, diameter, and also root-mean-square roughness of the surface, whereas their depth decreased. This changing trend in morphology was probably due to the modification of the chain conformation of PSFQs, which was influenced by the quality of the mixed solvents.^{29,32}

Moreover, a higher charge density in PSFQ2 determined the appearance of nodules, as illustrated in Figure 5(a,b).

On the other hand, the presence of water as a nonsolvent in solutions used for casting membranes influenced the AFM images; increasing the water content led to lower area pores for both polymer membranes under study [Fig. 4(c,d) for the PSFQ1 membranes and Fig. 5(c,d) for the PSFQ2 membranes] and to a lower number of nodules in the

TABLE II
Pore Characteristics Including the Area, Volume, Depth, and Diameter and Surface Roughness Parameters Including the Root-Mean-Square Roughness (rms), Nodule Height from the Height Profile (nhp), and Nodule Average Height from the Histogram (nhh) of Membranes Prepared from the PSFQs with Different Solvent Mixtures

Sample	Cast solvent	Pore characteristics				Surface roughness		
		Area (μm^2)	Volume (μm^3)	Depth (nm)	Diameter (μm)	rms (nm)	nhp (nm)	nhh (nm)
PSFQ1	60/40 DMF/MeOH	0.499	74.72	237.62	0.793	12.36	279	253
	20/80 DMF/MeOH	1.441	83.47	88.54	1.350	18.36	205	180
	60/40 DMF/water	0.342	8.85	46.21	0.665	8.83	170	135
	40/60 DMF/water	0.165	4.60	45.74	0.460	6.53	200	190
PSFQ2	60/40 MeOH/DMF	0.186	1.00	6.82	0.489	5.45	66	50
	20/80 MeOH/DMF	0.216	0.88	6.99	0.528	5.62	64	42
	60/40 MeOH/water	0.485	5.84	20.07	0.783	9.72	104	50
	20/80 MeOH/water	0.145	0.25	3.01	0.431	2.72	45	30

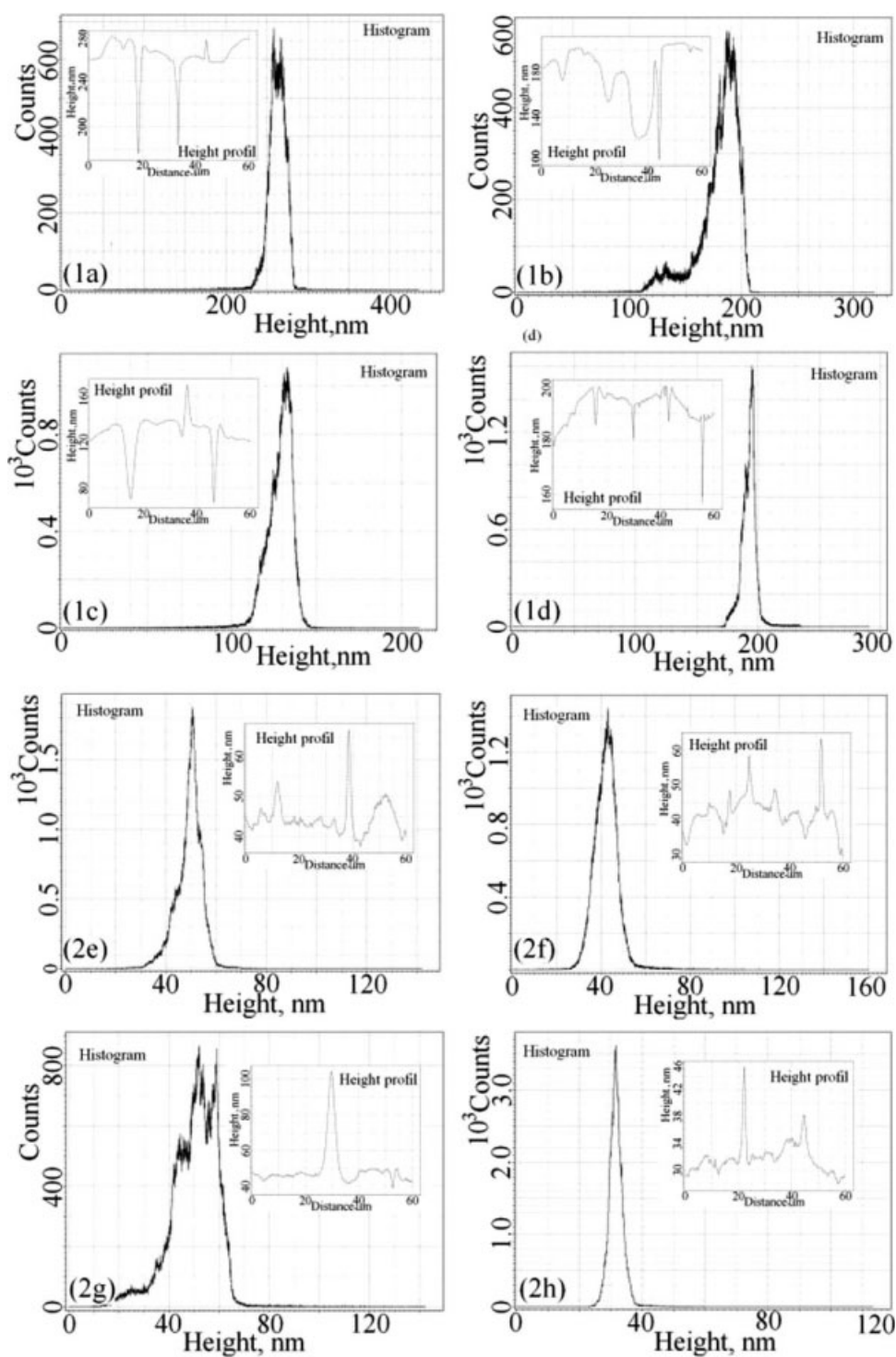


Figure 6 Histogram and surface profile (small plot) taken along a line from 2D AFM images: (1) PSFQ1 membranes: (a) Figure 3(1d), (b) Figure 3(2d), (c) Figure 4(c), and (d) Figure 4(d) and (2) PSFQ2 membranes: (e) Figure 5(a'), (f) Figure 5(b'), (g) Figure 5(c'), and (h) Figure 5(d').

PSFQ2 membranes [Fig. 5(c,d)]. Also, it may be assumed that the association phenomena of MeOH and water over different composition domains of their mixtures might have been one of the factors affecting the morphology of the PSFQ2 membrane surface. Thus, mixed solvents were formed

from water and MeOH associated with water at high water contents; in contrast, at high MeOH compositions, the mixtures consisted largely of MeOH and water associated with MeOH. These phenomena changed the PSFQ2 solubility and determined the modification of the solution properties,¹⁸

TABLE III
Total Surface Tension (γ_{sv}^d), Disperse Component (γ_{sv}^d),
Polar Component (γ_{sv}^p), and Contribution of the
Polar Component to the Total Surface
Tension ($\gamma_{sv}^p/\gamma_{sv}$) for the PSFQs²⁸

Sample	γ_{sv}^d	γ_{sv}^p	γ_{sv} (mN/m)	$\gamma_{sv}^p/\gamma_{sv}$ (%)
PSFQ1	8.12	29.88	38.00	78.63
PSFQ2	8.04	31.11	39.14	79.47

according to Figures 1 and 2, and the morphology [Fig. 5(c,d)].

Table II gives the average values of the pore characteristics and surface roughness parameters of membranes prepared from different solvent/nonsolvent mixtures, as identified in Figure 6. On the other hand, obviously, the number of nodules from the AFM images of the PSFQ2 membranes increased as the nonsolvent content increased.

Previous data²⁸ analyzed the hydrophilic/hydrophobic character of these polymers by means of surface tension parameters determined by the geometric mean method, with different test liquids considered. Table III shows that, when the polar component was higher than the disperse component of surface tension, the studied samples had a hydrophilic character; hydrophilicity increased from PSFQ1 to PSFQ2 because of the increasing molar volume of DMEA substituent groups, which involved a higher charge density. The wettability tendency observed from the contact angle of water with the polymers and the values obtained for the free energy of hydration confirmed the predominant hydrophilic character of the samples, with satisfactory values for different applications, for example, as semipermeable membranes. Also, a more pronounced hydrophilic character in the PSFQ2 sample was evidenced by AFM images (Fig. 5), in which the hydrophilic ionic domains were more obvious.

Antimicrobial activity assessments

The literature shows that quaternary ammonium salts represent one of the most popular types of antimicrobial agents.^{16,33–35} Their biological activity, depending on their structure and physicochemical properties, affects the interaction with the cytoplasmic membrane of bacteria and influences their cell metabolism.

The antimicrobial activity of PSFQs with various ionic chlorine contents, in DMSO, at different concentrations, was investigated against *E. coli* and *S. aureus*. As shown in Figure 7 and Table IV, these polymers inhibited the growth of microorganisms, with the inhibition becoming stronger with increasing polycationic nature of the modified PSF and

with polymer solution concentration. Also, for all solutions, the inhibition was intense compared to DMSO, which was used as a control sample.

The cationic PSFs modified with quaternary ammonium group interfered with the bacterial metabolism by electrostatic stacking at the cell surface of the bacteria.³⁵ This conclusion was evaluated in terms of the diameter of the inhibition zone, presented in Table IV. The results show that the bacterial activity of the tested compounds was dependent on the microorganism nature. Thus, *E. coli* was found to be much more sensitive to the investigated polymers than *S. aureus*.

On the other hand, the differences in the composition of the cell wall of Gram-negative (*E. coli*) and Gram-positive (*S. aureus*) bacteria cause different resistances to killing by antimicrobial agents. It is known that the component of Gram-positive bacteria cell walls is peptidoglycan, whereas the major constituents of Gram-negative bacteria cell walls are peptidoglycan together with other membranes, such as lipopolysaccharides and proteins. These components of the cell walls generate the hydrophilic character of *E. coli* bacteria and the hydrophobic character of *S. aureus*. Thus, the different inhibiting effects of PSFQ1 and PSFQ2 on the growth of the tested *E. coli* and *S. aureus* bacteria may have been due to different antimicrobial activities.

Therefore, all these aspects indicate that the antimicrobial activity depended not only on the substituent groups of the PSFQs but also on the hydrophilic or hydrophobic character of the bacteria, which generated different interactions of the quaternary ammonium salt groups with the bacterial cell membrane. In particular, the adhesion of the relatively hydrophilic *E. coli* to the hydrophilic PSFQs was higher than the adhesion of hydrophobic *S. aureus* cells.

CONCLUSIONS

In this article, we discuss the surface properties of some new PSFQs obtained by quaternization of CMPSF with DMEA. For the AFM study, all of the PSFQ membranes were prepared by a dry-cast process in different solvent/nonsolvent mixtures, DMF/MeOH, DMF/water, MeOH/DMF, and MeOH/water, which were selected as a function of the ionic chlorine content of PSFQ. The type of nonsolvents significantly influenced membrane morphology. The AFM images showed that the morphology of the membranes changed because of charge densities of PSFQ and the solvent/nonsolvent content:

- The ordered domains depended on the charge density of the polyelectrolytes and also on the history of the formed membranes.

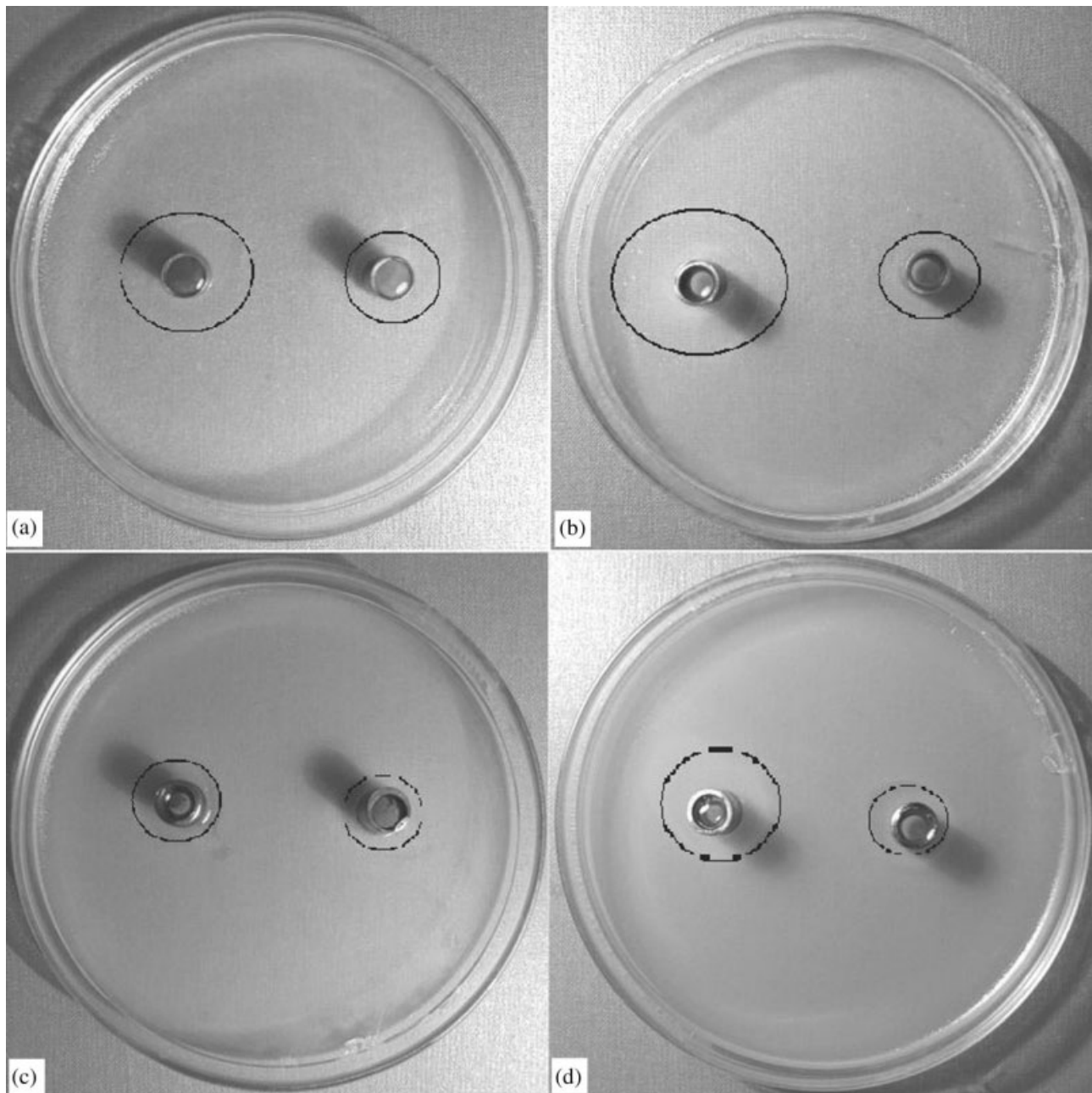


Figure 7 Antimicrobial screening tests: (a) PSFQ1 in DMSO, concentration = 1.08 g/L, against *E. coli*; (b) PSFQ2 in DMSO, concentration = 1.10 g/L, against *E. coli*; (c) PSFQ1 in DMSO, concentration = 1.08 g/L, against *S. aureus*; and (d) PSFQ2 in DMSO, concentration = 1.10 g/L, against *S. aureus*. In each figure, the inhibition area on the right side was recorded for DMSO as a control sample.

TABLE IV
Antimicrobial Activity Expressed by the Diameter of the Inhibition Zone (mm) of PSFQ1 and PSFQ2 in DMSO at Two Concentrations and of DMSO Used as a Control Sample Against *E. coli* and *S. aureus*

Microorganism	PSFQ1		PSFQ2		Control (DMSO)
	0.52 g/L	1.08 g/L	0.52 g/L	1.1 g/L	
<i>E. coli</i>	13	19	22	23	12
<i>S. aureus</i>	11	13	15	18	10

- The average size of the pores from AFM images increased with the nonsolvent content in the order MeOH, water for PSFQ1 and DMF, water for PSFQ2, respectively.
- The occurrence of nodules was intensified by the charge density of the polymers, especially in membranes obtained from solution in organic solvent/organic nonsolvent mixtures, and it was diminished in organic solvent/water mixtures.
- One may also consider that the interactions and association phenomena of MeOH and water over different composition domains of their mixtures should be among the factors affecting the morphology of the PSFQ2 membrane surface.

Thus, the results of the dilute solution study for PSFQ showed that intrinsic viscosity and preferential adsorption were modified, so that solubility increased in the order DMF/water, DMF/MeOH for PSFQ1 and MeOH/DMF, MeOH/water for PSFQ2. This indicated that the intrinsic viscosity value of a charged polymer solution is an important variable governing the morphology of membranes and also that chain association in a polymer solution results in macromolecular aggregates and influences surface topology.

The antimicrobial activity of PSFs with quaternary ammonium groups is considered to be one of the important properties that are directly related to new possible applications. In this study, the adhesion of *E. coli* and *S. aureus* cells to PSFQ was investigated. These polymers inhibited the growth of microorganisms, with inhibition becoming stronger with the increasing polycationic nature of the modified PSF and the concentration of the polymer solution. Moreover, the adhesion of the relatively hydrophilic *E. coli* to hydrophilic PSFQ was higher than the adhesion of the hydrophobic *S. aureus* cells.

References

1. Barikani, M.; Mehdipour-Ataei, S. *J Polym Sci Part A: Polym Chem* 2000, 38, 1487.
2. Väisänen, P.; Nyström, M. *Acta Polytech Scand* 1997, 247, 25.
3. (a) Higuchi, A.; Iwata, N.; Tsubaki, M.; Nakagawa, T. *J Appl Polym Sci* 1988, 36, 1753; (b) Higuchi, A.; Nakagawa, T. *J Appl Polym Sci* 1990, 41, 1973; (c) Higuchi, A.; Koga, H.; Nakagawa, T. *J Appl Polym Sci* 1992, 46, 449.
4. Johnson, R. N. In *Encyclopedia of Polymer Science and Technology*; Herman, F. M.; Norman, G. G.; Bikales, M. N., Eds.; Wiley: New York, 1969; Vol. 11, p 447.
5. Huang, R. Y. M.; Shao, P.; Burns, C. M.; Feng, X. *J Appl Polym Sci* 2001, 82, 2651.
6. Sluma, H. D.; Huff, D. U.S. Pat. 5,013,765 (1991).
7. Higuchi, A.; Shirano, K.; Harashima, M.; Yoon, B. O.; Hara, M.; Hattori, M.; Imamura, K. *Biomaterials* 2002, 23, 2659.
8. Tomaszewska, M.; Jarosiewicz, A.; Karakulski, K. *Desalination* 2002, 146, 319.
9. Savariar, S.; Underwood, G. S.; Dickinson, E. M.; Schielke, P. J.; Hay, A. S. *Desalination* 2002, 144, 15.
10. Sotiropoulos, K.; Pispas, S.; Hadjichristidis, N. *Macromol Chem Phys* 2004, 205, 55.
11. Ismail, A. F.; Hafiz, W. A. *J Sci Technol* 2002, 24, 815.
12. Lu, Z.; Liu, G. *Macromolecules* 2004, 37, 174.
13. M'Bareck, C. O.; Nguyen, Q. T.; Alexandre, S.; Zimmerlin, I. *J Membr Sci* 2006, 278, 10.
14. Huang, Y.; Xiao, C. *Polymer* 2007, 48, 371.
15. Guan, R.; Zou, H.; Lu, D.; Gong, C.; Liu, Y. *Eur Polym J* 2005, 41, 1554.
16. Yu, H.; Huang, Y.; Ying, H.; Xiao, C. *Carbohydr Polym* 2007, 69, 29.
17. Ioan, S.; Filimon, A.; Avram, E. *J Appl Polym Sci* 2006, 101, 524.
18. Filimon, A.; Avram, E.; Ioan, S. *J Macromol Sci Phys* 2007, 46, 503.
19. Idris, A.; Zain, N. M. *J Teknol* 2006, 44, 27.
20. Kochkodan, V.; Tsarenko, S.; Potapchenko, N.; Kosinova, V.; Goncharuk, V. *Desalination* 2008, 220, 380.
21. Guiver, M. D.; Black, P.; Tam, C. M.; Deslandes, Y. *J Appl Polym Sci* 1993, 48, 1597.
22. Avram, E.; Butuc, E.; Luca, C. *J Macromol Sci Pure Appl Chem* 1997, 34, 1701.
23. Avram, E. *Polym Plast Technol Eng* 2001, 40, 275.
24. Luca, C.; Avram, E.; Petrariu, I. *J Macromol Sci Chem* 1988, 25, 345.
25. Ghimici, L.; Avram, E. *J Appl Polym Sci* 2003, 90, 465.
26. Ioan, S.; Filimon, A.; Avram, E. *Polym Eng Sci* 2006, 46, 827.
27. Ioan, S.; Filimon, A.; Avram, E. *J Macromol Sci Phys* 2005, 44, 129.
28. Ioan, S.; Filimon, A.; Avram, E.; Ioanid, G. *e-Polymers* 2007, No. 031.
29. Qian, J. W.; An, Q. F.; Wang, L. N.; Zhang, L.; Shen, L. *J Appl Polym Sci* 2005, 97, 1891.
30. Huang, D. H.; Ying, Y. M.; Zhuang, G. Q. *Macromolecules* 2000, 33, 461.
31. Hopkins, A. R.; Rasmussen, P. G.; Basheer, R. A. *Macromolecules* 1996, 297, 838.
32. Kesting, R. E. *J Appl Polym Sci* 1990, 41, 2739.
33. Hazziza-Laskar, J.; Helary, G.; Sauvet, G. *J Appl Polym Sci* 1995, 58, 77.
34. Merianos, J. J. In *Disinfection, Sterilization and Preservation*; Block, S. S., Ed.; Lea & Febiger: Philadelphia, 1991; p 225.
35. Xu, X.; Li, S.; Jia, F.; Liu, P. *Life Sci J* 2006, 3, 59.